First passage time statistics of Brownian motion with purely time dependent drift and diffusion

A. Molini [a,b,*], P. Talkner [c], G.G. Katul [b,a], A. Porporato [a,b]

[a] *Department of Civil and Environmental Engineering, Pratt School of Engineering, Duke University, Durham, NC, USA*

[b] *Nicholas School of the Environment, Duke University, Durham, NC, USA*

[c] *Institut für Physik, Universität Augsburg, Augsburg, Germany*

1. Introduction

A wide range of geophysical and environmental processes occur under the influence of an external time-dependent and random forcing. Climate-driven phenomena, such as plant productivity [1], steno-thermal populations dynamics [2], crop production [3], the alternation between snow-storage and melting in mountain regions [4,5], the life cycle of tidal communities [6–8], and water-borne diseases outbreaks [9,10] offer a few such examples. In particular, several environmental systems can be described by state variables representing the availability of a resource whose dynamics is forced by diverse environmental factors and climatic oscillations. Elevated regions water availability — mainly originating from the melting of snow masses accumulated during the winter period (under the forcing of increasing temperatures), and precipitation (moving from the solid precipitation to the rainfall regime) — offers a relevant case study (presented in Section 4). All of these processes are now receiving increased attention in several branches of ecology, climate sciences and hydrology, due to their inherent sensitivity to climatic variability.

Analogous dynamical patterns can be found in slowly-driven, non-equilibrium systems with self organized criticality (*SOC*), where the density of potentially relaxable sites in the system can be described via a random walk with time-dependent drift and diffusion terms [11–13]. In these systems, the time dependence in the diffusion term derives from a gradual

* Corresponding author at: Department of Civil and Environmental Engineering, Pratt School of Engineering, Duke University, Durham, NC, USA. Tel.: +1 919 668 3809; fax: +1 919 684 8741.

E-mail address: annalisa.molini@duke.edu (A. Molini).

decrease of susceptible sites, so that sites availability acts on the directionality and pathways (drift term) of the "avalanches" until diffusion "kills" all the activity in the system [14, pp. 120–131]. Similar dynamics occur in systems displaying stochastic resonance, where noise becomes modulated by an external periodic forcing (see [15–18] and references therein).

In many instances, the above-mentioned processes are restricted to the positive semi-axis or to the time at which a certain critical threshold is reached, and are represented by a Fokker–Planck (FP) equation with an absorbing barrier. The main focus here is on the first passage time statistics of the process, such as the survival probabilities and the first passage time densities. In the following, a brief review of the general properties of the time-dependent drift and diffusion processes with an absorbing barrier is presented. For constant drift and diffusion, the conditional probabilities are usually obtained via the method of images due to Lord Kelvin (see [19, p. 340]). The applicability of this method to the solution of time-dependent problems and its limitations are discussed and a necessary and sufficient criterion is formulated in Section 2.2. The analysis is then extended to different functional forms of the time-dependent drift and diffusion terms. Section 3.1 shows the analytical results for the first passage time statistics for a power-law time dependent drift and diffusion, while time-periodic drivers are analyzed in Section 3.2 (see [20–22] and references therein, for a more comprehensive review of periodically-driven stochastic processes). Finally, in Section 4, we present a stochastic model of the total mountain water equivalent during the apex phase of the melting season, incorporating both temperature effects and snow-precipitation input in the form of a power-law time-dependent Bm with an absorbing boundary.

2. Modeling framework

When a time-dependent random forcing is the dominant driver of the dynamics, a general representation for the state variable $x(t)$ can be formulated in the form of a stochastic differential equation given by

$$\mathrm{d}x(t) = \mu(t)\,\mathrm{d}t + \sigma(t)\,\mathrm{d}W(t) \tag{1}$$

where $\mu(t)$ and $\sigma(t)$ are purely time-dependent drift and diffusion terms, and $W(t)$ is a Wiener process with independent and identically Gaussian distributed (i.i.d.) increments $W(t) - W(s) \sim \mathcal{N}(0, t-s)$ for all $t \geqslant s \geqslant 0$. By assuming $t_0 = 0$, the solution of (1) takes the form

$$x(t) = x_0 + \int_0^t \mu(s)\mathrm{d}s + \int_0^t [\sigma(s)\mathrm{d}W(s)] \tag{2}$$

where t is time and $x_0 = x(0)$ can be either a random or a non-random initial condition independent of $W(t) - W(0)$. The associated FP equation describing the evolution of the probability density function (pdf) of $x(t)$ can be expressed as

$$\frac{\partial p(x,t|x_0)}{\partial t} = -\mu(t)\frac{\partial p(x,t|x_0)}{\partial x} + \frac{1}{2}\sigma^2(t)\frac{\partial^2 p(x,t|x_0)}{\partial x^2}, \tag{3}$$

where $p(x,t|x_0)$ is the transition pdf with initial condition $\delta(x - x_0)$ at t_0. Eq. (3) can also be expressed as a continuity equation for probability

$$\frac{\partial}{\partial t}p(x,t|x_0) = -\frac{\partial}{\partial x}j(x,t|x_0), \tag{4}$$

where

$$j(x,t|x_0) = \mu(t)p(x,t|x_0) - \frac{1}{2}\sigma^2(t)\frac{\partial p(x,t|x_0)}{\partial x}, \tag{5}$$

is the probability current (or flux) and $p(x,t|x_0)$ is the conditional probability. The solution of the FP equation in (3), is usually approached numerically (see for e.g., [23]). Whether this equation is analytically solvable for different functional forms of $\mu(t)$ and $\sigma(t)$ with an absorbing boundary, and whether these solutions can be applied in the study of the first passage statistics at such boundary is the main focus of this work. Case studies that employ these solutions are also presented.

2.1. Solution with natural boundaries

Consider first the solution of the FP equation (3) in the unbounded case. Given that the drift and diffusion coefficients depend only on time, the parabolic Eq. (3) can still be reduced to a constant-coefficient equation of the form

$$\frac{\partial p(z,\tau)}{\partial \tau} = \frac{\partial^2 p(z,\tau)}{\partial z^2} \tag{6}$$

by transforming the original variables x and t into

$$\tau = \frac{1}{2}\int \sigma^2(t)\mathrm{d}t + A \tag{7}$$

and

$$z = x - \int \mu(t)\mathrm{d}t + B \tag{8}$$

where A and B are generic constants. The solution with natural boundaries is then $p(z,\tau) = \frac{1}{2\sqrt{\pi\tau}} \exp\left(-\frac{z^2}{4\tau}\right)$ [24]. Hence, given the initial condition

$$p(x, 0|x_0) = \delta(x - x_0), \tag{9}$$

the following normalized solution for an unrestricted process, starting from x_0, can be obtained as

$$p_u(x, t|x_0) = \frac{1}{2\sqrt{\pi S(t)}} \exp\left(-\frac{(x - x_0 - M(t))^2}{4S(t)}\right), \tag{10}$$

where, assuming the integrability of $\mu(t)$ and $\sigma(t)$,

$$M(t) = \int_0^t \mu(s)\mathrm{d}s \tag{11}$$

and

$$S(t) = \frac{1}{2}\int_0^t \sigma^2(s)\mathrm{d}s. \tag{12}$$

It should be noted that the transformation in Eqs. (8) and (7) also applies to any boundary condition imposed at a finite position. Therefore, as will be seen, it is not directly helpful in solving first passage time problems, as in that case it would lead to a problem with *moving* absorbing boundary conditions.

2.2. First passage time distributions

For a Bm process commencing at a generic position x_0 at $t = 0$, the time at which this process reaches an arbitrary threshold a for the first time (first passage time) is itself a random variable whose statistics are fundamental in many branches of science such as chemistry, neural-sciences and econometrics. In the following, it is assumed that the process is starting at a certain state $x_0 > 0$ and that it is bounded to the positive semi-axis via an absorbing barrier $x = 0$. This hypothesis does not imply any loss of generality, considering that the solution of Eq. (3) with an absorbing boundary condition only depends on the distance of the initial point x_0 from the threshold, but not separately on x_0 and the threshold position. Eq. (3) is then solved with the boundary condition

$$p(0, t) = 0, \tag{13}$$

and the additional condition of $x = +\infty$ being a natural boundary to ensure that $j(+\infty, t|x_0) = 0$. For such a system, the survival probability $F(t|x_0)$ is defined as the probability of the process trajectories not absorbed before time t, i.e.

$$F(t|x_0) = \int_0^{+\infty} p(x, t|x_0)\,\mathrm{d}x \tag{14}$$

and the first passage probability density $g(t|x_0)$ is either the "rate of decrease" in time of F

$$g(t|x_0) = -\frac{\partial}{\partial t}F(t|x_0)\,. \tag{15}$$

or, alternatively, the negative probability current at the boundary

$$g(t|x_0) = \left.\frac{\sigma^2(t)}{2}\frac{\partial}{\partial x}p(x, t|x_0)\right|_{x=0}, \tag{16}$$

since $p(0, t|x_0) = 0$ from (13).

2.3. Method of images in time-dependent systems

When the drift and diffusion terms are independent of t and x, Eq. (3) with absorbing boundaries can be readily solved by the method of images, often adopted in problems of heat conduction and diffusion [25,26,14,27]. This method can also be used for solving boundary-value problems for a Bm with particular forms of time-dependent drift and diffusion. The basic premise of this method is that given a linear PDE with a point source (or sink) subject to homogeneous boundary conditions in a finite domain, its general solution can be obtained as a superposition of many 'free space' solutions (i.e. disregarding the boundary conditions) for a number of virtual sources (i.e. outside the domain) selected so as to obtain the correct boundary condition. The image source (or sink) is placed as mirror image of the original source (or sink) from the boundary with a strength or intensity selected to match the boundary condition.

Consider Eq. (3) with the conditions (9) and (13). To solve this problem with the method of images, the barrier at 0 is replaced by a mirror source located at a generic point $x = y$, with $y < 0$ such that the solutions of the Fokker–Planck equation emanating from the original and mirror sources exactly compensate each other at the position of the barrier at each instant of time [14]. This implies the initial conditions in (9) must now be modified to

$$p(x, 0) = \delta(x - x_0) - \exp(-\eta)\,\delta(x - y), \tag{17}$$

where η determines the strength of the mirror image source. Due to the linearity of the FP equation, the solution in the presence of the initial condition (17) is the superposition of elementary solutions

$$p(x,\, t|x_0) = p_u(x,\, t|x_0) - \exp(-\eta)\, p_u(x,\, t|y). \tag{18}$$

Since the condition (13) requires that $p(0,\, t|x_0) = 0$, one obtains that

$$\frac{(M(t)+x_0)^2}{4S(t)} = \eta + \frac{(M(t)+y)^2}{4S(t)} \tag{19}$$

for all $t > 0$. By assuming $t = 0$, we have $x_0^2 = y^2$ and recalling that $y < 0$, the resulting image position is $-x_0$. This, inserted again in Eq. (19), yields

$$\frac{M(t)}{S(t)} = \frac{\eta}{x_0} = q, \tag{20}$$

where the constant q is analogous to the Péclet number of the process—i.e. the ratio between the advection and diffusion rates [14].

After differentiating (20) with respect to t, it is seen that the method of images requires that the drift and the diffusion terms be proportional to each other. Namely, the intensity η of the image source must be constant in time. In fact, only in this case it is still possible to transform the original time scale into a new one, for which the transformed process is governed by time-independent drift and diffusion terms. Hence, writing the drift and diffusion terms as

$$\mu(t) = kh(t) \quad \text{and} \quad \frac{\sigma^2}{2} = lh(t), \tag{21}$$

the associated FP equation is

$$\frac{\partial p}{\partial t} = h(t) \quad -k\frac{\partial}{\partial x} + l\frac{\partial^2}{\partial x^2} \quad p. \tag{22}$$

Transforming the original time t variable in

$$\tilde{\tau} = \int_0^t h(s)\mathrm{d}s \tag{23}$$

Eq. (22) finally becomes

$$\frac{\partial p}{\partial \tilde{\tau}} = \quad -k\frac{\partial}{\partial x} + l\frac{\partial^2}{\partial x^2} \quad p. \tag{24}$$

This condition is valid for any time-dependent diffusion when the drift is identically vanishing. Assuming the proportionality in (20) between $\mu(t)$ and $\sigma(t)$, the general solution for (3) under conditions (9) and (13) can be written as

$$p(x,\, t|x_0) = \frac{1}{2\sqrt{\pi S(t)}} \quad \exp \quad -\frac{(x - x_0 - M(t))^2}{4S(t)} \quad - \exp(-x_0 q) \exp \quad -\frac{(x + x_0 - M(t))^2}{4S(t)} \quad , \tag{25}$$

provided $M(t) = qS(t)$. Substituting for constant drift and diffusion in (25) one recovers the well-known solution for a biased Bm [25]

$$p(x,\, t|x_0) = \frac{1}{\sqrt{2\pi}\sqrt{\sigma^2 t}} \quad \exp \quad -\frac{(x_0 - x + \mu t)^2}{2\sigma^2 t} \quad - \exp \quad -\frac{2x_0\mu}{\sigma^2} \quad \exp \quad \frac{(x + x_0 - \mu t)^2}{2\sigma^2 t} \tag{26}$$

with survival function $F(t|x_0)$ given by

$$F(t|x_0) = \Phi \quad \frac{\mu t + x_0}{\sigma\sqrt{t}} \quad - \exp \quad -\frac{2x_0\mu}{\sigma^2} \quad \Phi \quad \frac{\mu t - x_0}{\sigma\sqrt{t}} \quad , \tag{27}$$

where Φ is the standard normal integral, and first passage time distribution

$$g(t|x_0) = \frac{x_0}{\sigma\sqrt{2\pi}t^{3/2}} \exp \quad -\frac{(x_0 + \mu t)^2}{2\sigma^2 t} \quad . \tag{28}$$

Eq. (28) is the Wald (or inverse Gaussian) density function, that for a zero drift becomes of order $t^{-3/2}$ as $t \to +\infty$ (the first passage time has no finite moments for pure diffusion).

Similarly, the solution to the FP in Eq. (3) with a reflecting boundary at $x = 0$ can be obtained by the method of images provided that drift and diffusion are proportional to each other. The solution then becomes

$$\begin{aligned} p(x,\, t|x_0) = & \frac{1}{2\sqrt{\pi S(t)}} \quad \exp \quad -\frac{(x - x_0 - M(t))^2}{4S(t)} \quad + \exp(-x_0 q) \exp \quad -\frac{(x + x_0 - M(t))^2}{4S(t)} \\ & - \quad \frac{1}{2}\frac{M(t)}{S(t)} \exp \quad \frac{x\eta}{x_0} \quad 1 - \mathrm{erf} \quad \frac{x + x_0 + M(t)}{2\sqrt{S(t)}} \quad , \end{aligned} \tag{29}$$

with $\frac{1}{2}\left[1-\text{erf}\ \frac{x+x_0+M(t)}{2\sqrt{S(t)}}\right]$ being the Q-function representing the tail probability of a Gaussian distribution. Eq. (29) generalizes the solution in Ref. [25] for a Bm with constant drift and diffusion and a reflecting boundary at 0.

3. Time dependent drift and diffusion

3.1. Power-law time dependence

As a first example of Bm with purely time-dependent drivers, the case of an unbiased diffusion ($q = 0$) and power-law time dependent diffusion term $\sigma^2(t) = 2At^\alpha$ and $\alpha > -1$ are considered. For this process, the conditional probability $p(x, t|x_0)$ with absorbing barriers at 0, takes on the form

$$p(x,t|x_0) = \frac{\sqrt{1+\alpha}}{2\sqrt{A\pi}}t^{-(\alpha+1)}\ \exp\ -\frac{t^{-(\alpha+1)}(x-x_0)^2(1+\alpha)}{4A}\ -\exp\ -\frac{t^{-(\alpha+1)}(x+x_0)^2(1+\alpha)}{4A}\quad, \tag{30}$$

while the survival function becomes

$$F(t|x_0) = \text{erf}\ \left.\frac{x_0(1+\alpha)^{\frac{1}{2}}}{2\sqrt{A}}t^{-\frac{\alpha+1}{2}}\right). \tag{31}$$

Fig. 1(a) shows the conditional probability (30) at a fixed time instance $t = 15$ time steps for $A = 15, x_0 = 50$, and $\alpha = -0.1$ (bold line) 0.5 (thin line), and 1 (dotted line). Given the asymptotic properties of the error function [28], the long-time behavior of $F(t|x_0)$ is then $\sim \frac{x_0(1+\alpha)^{1/2}}{2\sqrt{A}}t^{-\frac{\alpha+1}{2}}$, recovering for $\alpha = 0$ the $-1/2$ tail decay of an unbiased constant diffusion (see Fig. 1(b)). Also, by differentiating Eq. (31), one obtains

$$g(t|x_0) = \frac{x_0}{2\sqrt{\frac{A\pi}{(\alpha+1)^3}}t^{(3+\alpha)/2}}\exp\ -\frac{x_0(\alpha+1)t^{-(\alpha+1)}}{4A} \tag{32}$$

whose tail behaves as $\sim t^{-\frac{3+\alpha}{2}}$. Hence, Eq. (32) is an inverse Gaussian distribution — that for $\alpha = 0$ becomes an inverse Gamma distribution with shape parameter 1/2 [29, pp. 284–285]. These solutions characterize inter-arrival times between intermittent events when a system displays sporadic randomness [30–32].

The solutions in the case of proportional power-law diffusion and drift can be derived in an analogous manner. For $\mu(t) = qAt^\alpha$ and $\sigma(t) = \sqrt{2}A^{1/2}t^{\alpha/2}$, the conditional probability $p(x, t|x_0)$ takes the form

$$p(x,t|x_0) = \frac{\sqrt{\alpha+1}t^{-(\alpha+1)/2}}{2\sqrt{A\pi}}\left\{\exp\left[-\frac{(1+\alpha)t^{-(\alpha+1)}\left(-x+\frac{Aqt^{1+\alpha}}{1+\alpha}+x_0\right)^2}{4A}\right]\right.$$
$$\left. -\exp\left[-qx_0-\frac{(1+\alpha)t^{-(\alpha+1)}\left(x-\frac{Aqt^{1+\alpha}}{1+\alpha}+x_0\right)^2}{4A}\right]\right\} \tag{33}$$

and the survival function, now incorporating the drift contribution, can be written as

$$F(t|x_0) = \Phi\left\{t^{-\frac{(\alpha+1)}{2}}\frac{\left(Aqt^{\alpha+1}+x_0+x_0\alpha\right)}{2\sqrt{A(\alpha+1)}}\right\} - \exp\left(-qx_0\right)\Phi\left\{t^{-\frac{(\alpha+1)}{2}}\frac{\left(Aqt^{\alpha+1}-x_0-x_0\alpha\right)}{2\sqrt{A(\alpha+1)}}\right\}. \tag{34}$$

For positive q's, $F(t|x_0)$ tends in the long term to $1-\exp(-qx_0)$, while for negative q's, $F(t|x_0) \sim \frac{2\sqrt{\alpha+1}}{q\sqrt{A}}t^{-\frac{\alpha+1}{2}}\exp\ -\frac{q\sqrt{A}t^{\frac{\alpha+1}{2}}}{2\sqrt{\alpha+1}}$. This fact implies that the probability for a trajectory to be eventually absorbed is 1 for the biased process directed towards the barrier, and $\exp(-qx_0)$ when the bias is away from the barrier (infinite aging). When the state variable represents the availability of a resource in time, the sign of q determines if this resource is subject to continuous accumulation (positive q), or it undergoes a total depletion (negative q) with probability 1. Such a result is analogous to the one of a simple biased Bm with constant drift and diffusion [14], with the difference that in this case, $F(t|x_0)$ decays to 0 or $1-\exp(-qx_0)$ with a rate that is governed by α.

As an example, Fig. 1(c) and (d) respectively show a negatively biased power-law time-dependent Bm and a positively biased one for the same set of parameters in (b) and $q = -0.1$ and $q = 0.1$, for $A = 1, x_0 = 1$ and $\alpha = 0$ (constant diffusion, bold line), -0.5 (thin dotted line), 0.5 (dashed line), and 1 (thin line). As evident in panel (c), $F(t|x_0)$ presents a faster decay to zero with increasing α, while for the positively biased Bm in panel (d) the decay to the asymptotic value $1-\exp(-qx_0)$ is slower with decreasing α.

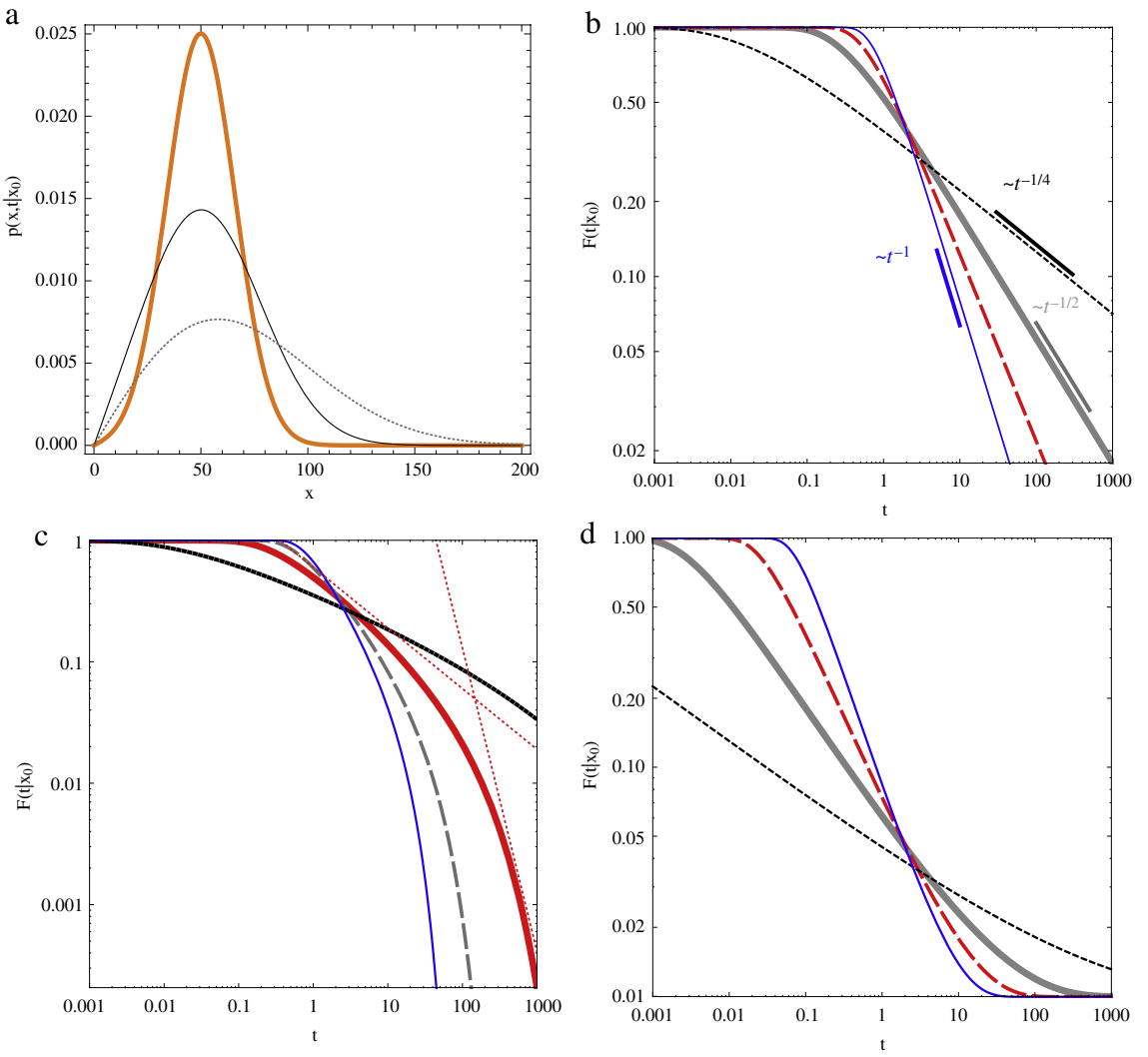

Fig. 1. Conditional probability $p(x, t|x_0)$ at different fixed times t (a) and survival function $F(t|x_0)$ (b) for the pure power-law time dependent process described in Section 3.1, together with $F(t|x_0)$ for the negatively biased power-law process (c) and for the positively biased one (d). Panel (a) represents $p(x, t|x_0)$ at a fixed time $t = 15$ steps for $A = 15$, $x_0 = 50$, and $\alpha = -0.1$ (bold line), $= 0.5$ (thin line), and $= 1$ (dotted line). In (b) $F(t|x_0)$ is displayed as a function of t for $A = 1$, $x_0 = 1$ and $\alpha = 0$ (constant diffusion, bold line), $\alpha = -0.5$ (thin dotted line), $\alpha = 0.5$ (dashed line), and $\alpha = 1$ (thin line). Panels (c) and (d) display respectively a negatively biased power-law time dependent Bm and a positively biased one for the same set of parameters in (b) and $q = -0.1$ and $q = 0.1$.

Finally, $g(t|x_0)$ can be obtained from (34) as

$$g(t|x_0) = \frac{x_0(1+\alpha)^{3/2}}{2\sqrt{\pi A}t^{\frac{3+\alpha}{2}}} \exp\left[-\frac{t^{-(\alpha+1)}\left(Aqt^{\alpha+1} + x_0 + \alpha x_0\right)^2}{4A(1+\alpha)}\right] \tag{35}$$

where for $\alpha = 0$ the decay of $g(t|x_0)$ recovers the constant diffusion $t^{-3/2}$-law for $t \to \infty$ and $q = 0$.

3.2. Periodic drift and diffusion

In this section, the case of a periodic diffusion in the form $\sigma^2(t) = [2A\cos(\omega t)]^2$ and $q = 0$ is considered. For periodically driven diffusion, the conditional probability can be derived in the form

$$p(x, t|x_0) = \left(\frac{\omega}{\pi\vartheta(t)}\right)^{\frac{1}{2}} \exp\left[-\frac{2\omega\left(x^2 + x_0\right)}{\vartheta(t)}\right]\left\{\exp\left[\frac{\omega(x+x_0)^2}{\vartheta(t)}\right] - \exp\left[\frac{\omega(x-x_0)^2}{\vartheta(t)}\right]\right. \tag{36}$$

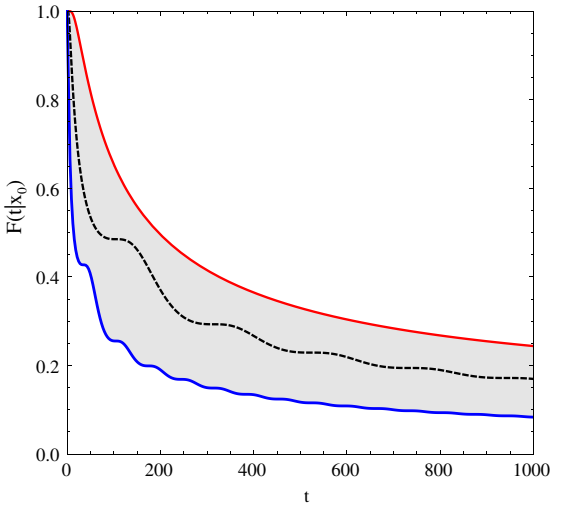

Fig. 2. Survival function $F(t|x_0)$ for the periodic purely diffusive process described in Section 3.2, and for $A = 15$ and $x_0 = 50$. Upper, dashed and lower curves represent F for $\omega = 0.0001$, $\omega = 0.015$, and $\omega = 0.045$, respectively.

where $\vartheta(t) = A^2[2\omega t + \sin(2\omega t)] > 0$. Thus, the solution becomes modulated in time with frequency ω. The survival probability is in turn

$$F(t|x_0) = \text{erf}\quad x_0\sqrt{\frac{\omega}{\vartheta(t)}}\quad , \tag{37}$$

that is represented in Fig. 2 for different values of the frequency ω. Finally, the first passage time density is an ω-modulated inverse Gaussian distribution

$$g(t|x_0) = \frac{4x_0A^2}{\sqrt{\pi}}\frac{\omega^{3/2}\cos(\omega t)^2}{\vartheta(t)^{3/2}}\exp\quad -\frac{\omega x_0^2}{\vartheta(t)}\quad . \tag{38}$$

In the case $q \neq 0$, the conditional probability $p(x, t|x_0)$ becomes

$$p(x, t|x_0) = \frac{\sqrt{\omega}}{\sqrt{\pi q\vartheta(t)}}\left\{\exp\left[-\frac{\omega\quad x_0 - x + \frac{q\vartheta(t)}{4\omega}}{\vartheta(t)}^2\right] - \exp\left[-qx_0 - \frac{\omega\quad x_0 + x - \frac{q\vartheta(t)}{4\omega}}{\vartheta(t)}^2\right]\right\}, \tag{39}$$

where, again, the absorption at the barrier represents a recurrent ($q < 0$) or a transient ($q > 0$) state, as was observed for the power-law drift and diffusion process in Section 3.1. The recurrent case is illustrated in Fig. 3 (b)–(d), where we report the time-position evolution of $p(x, t|x_0)$ as a function of increasing ω. From (39), given $\omega/\vartheta(t) > 0$, the expression for the survival function can be derived and takes the form

$$F(t|x_0) = \tfrac{1}{2}\left[1 + \text{erf}\left(\frac{q\vartheta(t)+4x_0\omega}{4\sqrt{\omega\vartheta(t)}}\right. \quad + \exp(-qx_0)\,\text{erfc}\quad \frac{q\vartheta(t)-4x_0\omega}{4\sqrt{\omega\vartheta(t)}}\quad - 2\exp(-qx_0)\right], \tag{40}$$

which, given the equality $\text{erfc}(-x) = 2 - \text{erfc}(x)$, can be alternatively expressed as

$$F(t|x_0) = \Phi\quad \frac{q\vartheta(t) + 4x_0\omega}{2\sqrt{2\omega\vartheta(t)}}\quad - \exp(-qx_0)\,\Phi\quad \frac{q\vartheta(t) - 4x_0\omega}{2\sqrt{2\omega\vartheta(t)}}\quad . \tag{41}$$

The first passage time density $g(t|x_0)$ is given by

$$g(t|x_0) = \frac{4A^2x_0}{\sqrt{\pi}}\frac{\omega^{3/2}\cos(\omega t)^2}{\vartheta(t)^{3/2}}\exp\quad -\frac{(q\vartheta(t) + 4x_0\omega)^2}{16\omega\vartheta(t)}\quad . \tag{42}$$

The method of images can also be applied to the solution of different forms of periodic drivers, such as the case $\mu(t) = q(B + A\cos(\omega t))$ and $\sigma(t) = \sqrt{2(B + A\cos(\omega t))}$, with $(B + A\cos(\omega t)) > 0$. In this last case, the drift term is the same as the one usually investigated in neuron dynamics by simple integrate-and-fire models displaying stochastic resonance (see for example the neuron dynamics case in [15,16]. In those models, the diffusion is usually constant so that the condition in Eq. (20) is not satisfied. Thus, it is often implied that $\mu(t) \ll \sigma^2/2$ approximately resembles a time dependent diffusion with drift identically vanishing or that $B \gg A$ (approximating the simpler constant drift and diffusion case). In these cases,

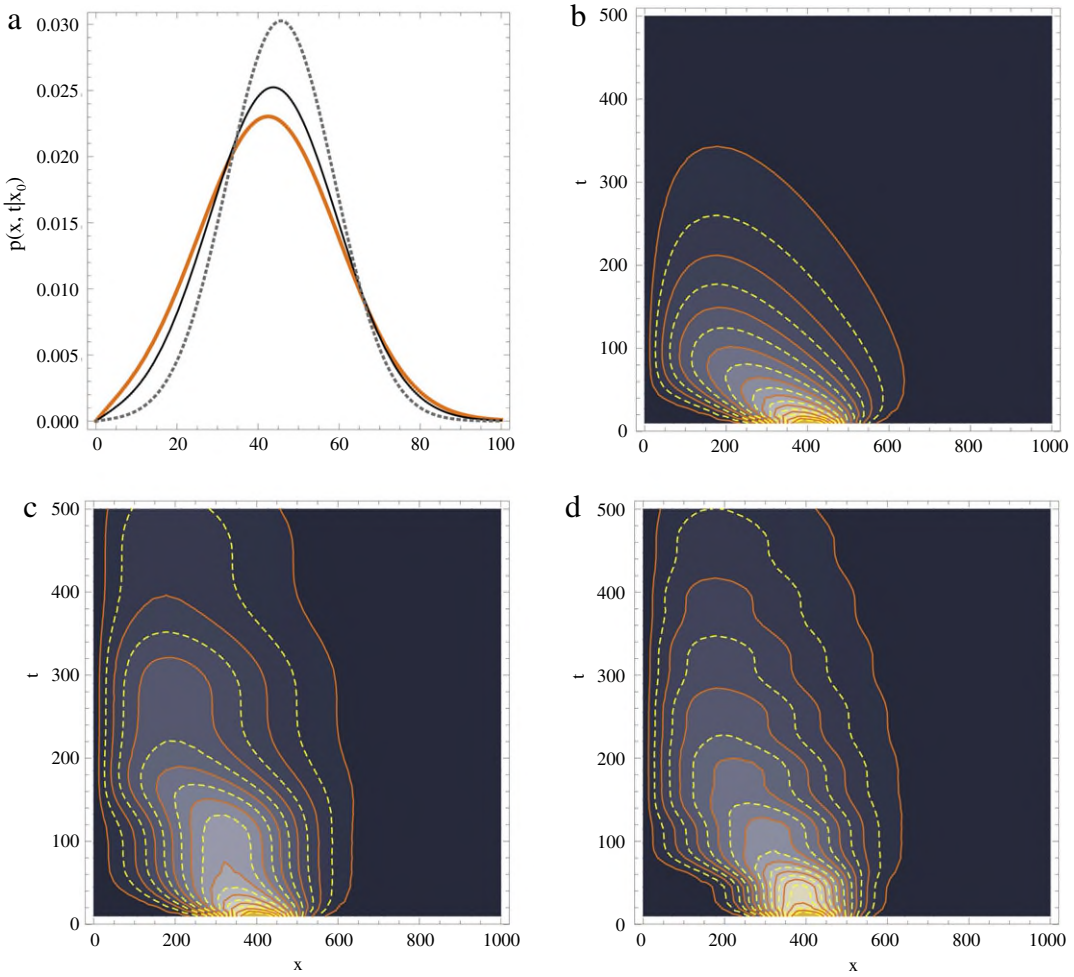

Fig. 3. Conditional probability $p(x, t|x_0)$ for the periodic negatively biased Bm described in Section 3.2. Panel (a) represents $p(x, t|x_0)$ at a fixed time $t = 3$ steps for $A = 15$, $x_0 = 50$, $q = -0.05$, and $\omega = 0.0001$ (bold line), $= 0.5$ (thin line), and $= 0.9$ (dotted line). Also, contour plots (b) to (d) show $p(x, t|x_0)$ for $A = 15$, $x_0 = 450$ and $q = -0.01$ as a function of x and t, for $\omega = 0.0001$ (panel (b)), $\omega = 0.015$ (panel (c)), and $\omega = 0.045$ (panel (d)) respectively. Note how the negative drift forces the probability mass toward the barrier.

the method of images only offers approximated solutions [15,16]). Specifically, for a time dependent (and periodic) drift $\mu(t) = B + A\cos(\omega t)$ and constant diffusion $\frac{1}{2}\sigma^2$, an approximation for $p(x, t|x_0)$ in the presence of an absorbing barrier at 0 can still be obtained by using the method of images conditional to the fact that $\mu(t) \ll \sigma^2/2$. Only by adopting this assumption in fact, we can obtain an (approximated) solution for the survival function by means of Eq. (25) although drift and diffusion are not strictly proportional to each other. In this way we find

$$F(t|x_0) = \frac{1}{2}\left\{\operatorname{erfc}\left(\frac{Bt + \frac{A\sin(\omega t)}{\omega} - x_0}{\sqrt{2}\sigma\sqrt{t}}\right) - \exp\left(\frac{2x_0(B\omega t + A\sin(\omega t))}{\sigma^2\omega t}\right)\operatorname{erfc}\left(\frac{Bt + \frac{A\sin(\omega t)}{\omega} + x_0}{\sqrt{2}\sigma\omega\sqrt{t}}\right)\right\} \tag{43}$$

and, analogous to [15], from Eq. (15) the first passage density can be expressed as

$$g(t|x_0) = \frac{x_0 \exp\left\{-\frac{\left[Bt + \frac{A\sin(\omega t)}{\omega} - x_0\right]^2}{2\sigma^2 t}\right\}}{\sqrt{2\pi}\sigma t^{\frac{3}{2}}} + \frac{A\exp\left\{\frac{[(x_0+Bt)\omega + A\sin(\omega t)]^2}{2\sigma^2\omega^2 t}\right\}\operatorname{erfc}\left(\frac{Bt + \frac{A\sin(\omega t)}{\omega} + x_0}{\sqrt{2}\sigma\sqrt{t}}\right)\left[t\cos(\omega t) - \frac{1}{\omega}\sin(t\omega)\right]}{\sigma^2 t^2}. \tag{44}$$

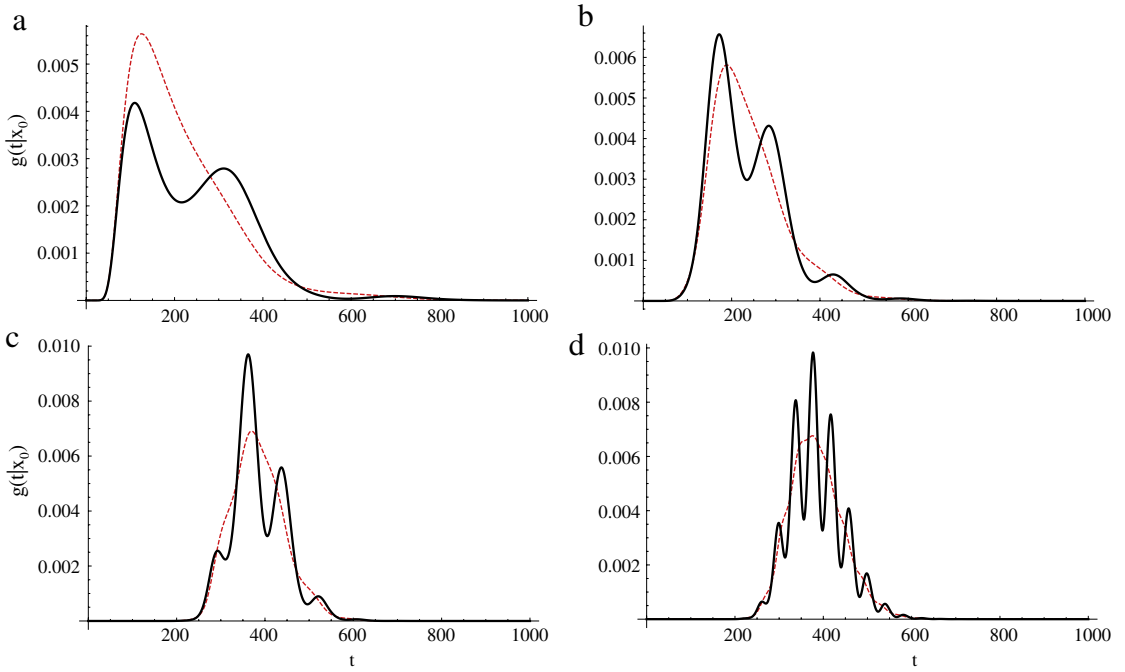

Fig. 4. First passage densities $g(t|x_0)$ (bold black line, Eq. (44)), and $\tilde{g}(t|x_0)$ (red dotted line, Eq. (45)), respectively for (a) $\mu = 0.065$, $\sigma = 0.5$, $x_0 = 25$, $A = 0.032$ and $\omega = 0.016$; (b) $\mu = 0.065$, $\sigma = 0.35$, $x_0 = 15.5$, $A = 0.025$ and $\omega = 0.04$; (c) $\mu = 0.065$, $\sigma = 0.2$, $x_0 = 25$, $A = 0.03$ and $\omega = 0.07$, and (d) $\mu = 0.065$, $\sigma = 0.2$, $x_0 = 25$, $A = 0.03$ and $\omega = 0.15$. The discrepancy between $\tilde{g}(t|x_0)$ and $g(t|x_0)$ clearly signifies the failure of the method of images for problems with time-dependent Péclet numbers. (For interpretation of the references to colour in this figure legend, the reader is referred to the web version of this article.)

The approximated nature of the solution is evidenced by the fact that, the image source intensity is no longer constant in time, so that by evaluating the probability current in 0 we obtain

$$\tilde{g}(t|x_0) = \frac{x_0}{\sqrt{2\pi}\sigma t^{3/2}} \exp\left\{-\frac{[\omega(Bt - x_0) + A\sin(\omega t)]^2}{2\omega^2\sigma^2 t}\right\}, \tag{45}$$

which is different from (44). In any case, the first passage time pdf in Eq. (44) is in good agreement with the numerical simulations in [15,16]. Also, when $A \to 0$ both the (44) and the (45) tend to the first passage time pdf for a simple biased Bm.

As highlighted in Fig. 4, when the magnitude of $\mu(t)$ becomes significant, the two pdfs diverge due to the losses of probability density at the barrier (Eq. (45)). For this reason, the method of images cannot be considered a general approach to solving problems described by Eq. (3) with a time-dependent Péclet number.

4. A case study: snowmelt dynamics

Snowmelt represents one of the paramount sources of freshwater for many regions of the world, and is sensitive to both temperature and precipitation fluctuations [33–38]. Snow dynamics is characterized by an accumulation phase during which snow water equivalent (i.e. the amount of liquid water potentially available by totally and instantaneously melting the entire snowpack) increases until a seasonal maximum h_0 is reached, followed by a depletion phase in which the snow mantle gradually decays (and releases the stored water content) due to the increasing air temperature. Such a dynamics is complex and its general description requires numerous physical parameters that are rarely measured or available. In this section, we focus on a stochastic model describing the total water equivalent from both snow and rainfall during the melting season, as forced/fed by both precipitation (moving from the solid to the liquid precipitation regime) and increasing air temperature.

Due to the simplified nature of our stochastic model, we will consider the total potential water availability (in terms of water equivalent) as the key variable, thus neglecting any further effects connected with snow percolation and metamorphism [39]. Snowfalls are here assumed to become more sporadic progressing into the warm season and the predominant controls over fresh water availability during the melting period are increasing air temperature and liquid precipitation. Accordingly, the melting phase is described by a power-law time dependent drift directed towards the total depletion of the snow mantle and by a power-law diffusion whose positive and negative excursions represent respectively precipitation events and pure melting periods. The melting process is often described by a linear function of time by using

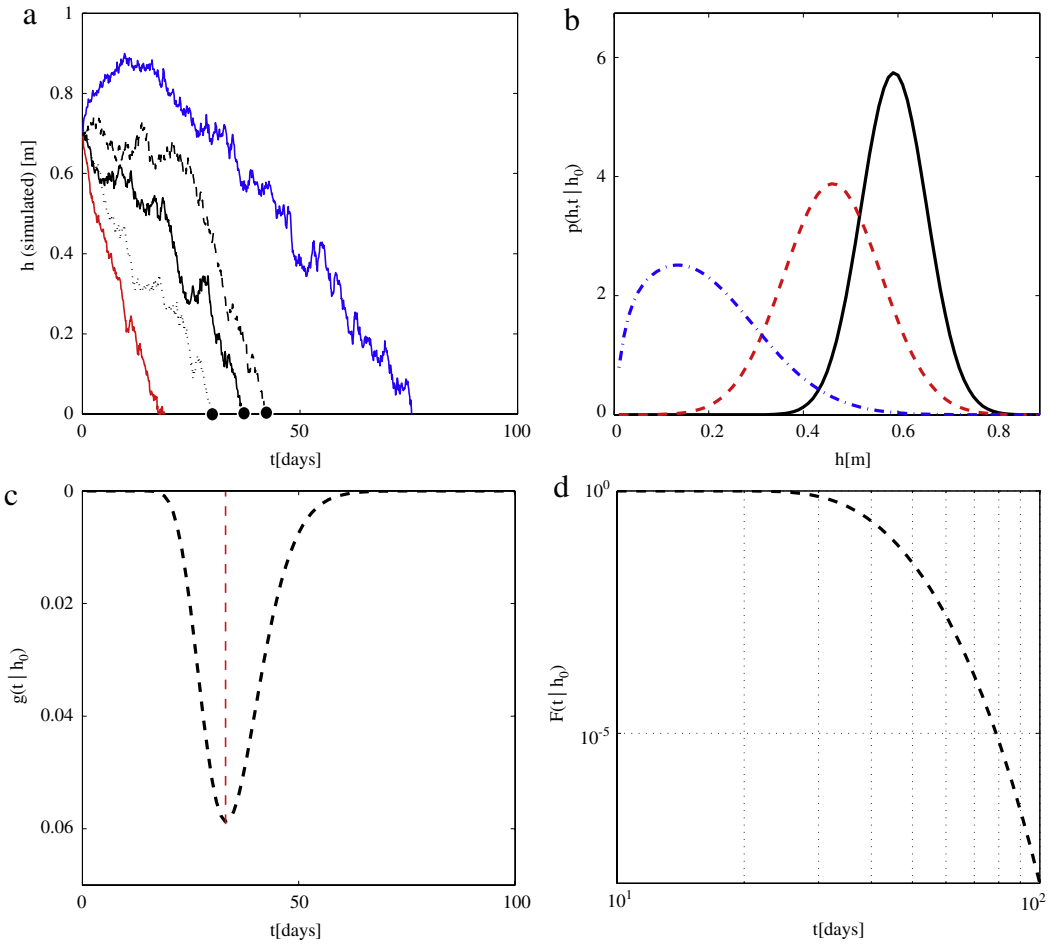

Fig. 5. Sample trajectories of specific water equivalent from elevated regions during the melting season (a), and analytical results for the coupled stochastic melting-precipitation process of Eq. (46) (panels (b) to (d)). Numerical results were obtained by simulating Eq. (46) by means of an Euler algorithm with step 10^{-2} days. Panel (a) shows a few sample trajectories of the process together with the curve of maximum values (upper curve) and minimum values (lower curve) over an ensemble of 10 000 simulations, for $\alpha = 0.25$ and $k = 0.24\ \mathrm{mm}^2/\mathrm{days}^\alpha$. Analytical results for the conditional probability $p(h, t|h_0)$ at different instants, the first passage time density $g(t|h_0)$, and the survival function $F(t|h_0)$, are also shown in panels (b)–(d).

the so called "degree-day" approach with time-varying melting-rate coefficients [39]. Considering that temperature varies seasonally and increases during the melting season, a power-law form for drift and diffusion during the spring season, still represents a parametrically-parsimonious and effective approximation of the basic driver of the process.

Under these assumptions, the dynamics of the total water equivalent depth for unit of area h — i.e. the amount of fresh water potentially available from both snow accumulation and rainfall [40] — at a given point in space can be can be reasonably described by the Langevin equation

$$\mathrm{d}h = -qkt^\alpha \mathrm{d}t + \sqrt{2kt^\alpha}\mathrm{d}W(t) \tag{46}$$

where k (with dimension $L^2/T^{\alpha+1}$) represents the accumulation/ablation rate. Note that here h includes both the rainfall and snowmelt contributions. Also, we hypothesize that both the drift and the diffusion scale with the same exponent α. This is a reasonable assumption given that variability of the process is expected to increase proceeding into the warm season. The initial condition is given by the snow water equivalent (SWE) h_0, accumulated during the cold season. The survival probability $F(t|h_0)$ for a given initial SWE and the first passage time density $g(t|h_0)$ can be respectively calculated from (34) and (35). Fig. 5 shows few sample trajectories of the process (panel (a)) obtained by the numerical simulation of Eq. (46) by means of a forward Euler algorithm with a time step of 10^{-2} days. The conditional probability $p(h, t|h_0)$ at different instants, the first passage time density $g(t|h_0)$, and the survival function $F(t|h_0)$, for the case $\alpha = 0.25$ and $k = 0.24\ \mathrm{mm}^2/\mathrm{days}^\alpha$ are also shown in panels (b)–(d). Here, we calibrated the parameters to obtain the mode of the first passage time at about 40 days after reaching the maximum SWE of the season h_0. The first passage time statistics presented offer important clues about the timing between melting and summer fresh-water availability under different climatic scenarios (consider for example the FPT pdf in Fig. 5(c)).

5. Conclusions

The first passage time properties of Brownian motion with purely time-dependent drift and diffusion coefficients subjected to an absorbing barrier were investigated. These processes can be used to mimic a variety of environmental and geophysical phenomena, representing the availability of a resource and its dynamics in time (e.g. the ablation phase of a snow mass accumulated during the winter period and forced by temperature and precipitation). Survival functions and pdfs for the first passage times at the barrier were derived for power-law and periodic forcing time-dependent drift and diffusion terms for the associated Fokker–Planck equation using the method of images. The general properties and limitations of this method were also reviewed, with reference to previous results obtained in the field of neural sciences and stochastic resonance. Particularly, we discussed how the applicability of the method of images to a Bm with time-dependent drift and diffusion is limited to the case of a process with constant Péclet number, i.e. with a time-independent ratio of drift and diffusion.

Where the time-dependence is of the power-law type, the derived first passage time density and survival functions share many analogies with the statistics of inter-arrival times between intermittent events when the considered system displays sporadic randomness. In the case of a periodic time-dependence, first passage time statistics appear to be modulated by the frequency of the forcing. The periodic forcing case has been also used to show the approximate nature of solutions obtained by the method of images, when time-dependent drift and diffusion terms are not linearly related. We finally show how a Bm with power-law decaying drift and diffusion can be used to describe the warm season dynamics of the total water equivalent in mountainous regions.

Acknowledgements

This study was supported, in part, by the National Science Foundation (NSF EAR 1063717, NSF-EAR 0628342, NSF-EAR 0635787 and NSF-ATM-0724088), and the Bi-national Agricultural Research and Development (BARD) Fund (IS-3861-96). We wish to thank Adi Bulsara for the helpful suggestions. We also thank Demetris Koutsoyiannis and the other three anonymous reviewers for their helpful suggestions.

References

[1] J. Ehleringer, T. Cerling, B. Helliker, C-4 photosynthesis, atmospheric CO2 and climate, Oecologia 112 (1997) 285–299.
[2] T. McClanahan, J. Maina, Response of coral assemblages to the interaction between natural temperature variation and rare warm-water events, Ecosystems 6 (2003) 551–563.
[3] C. Rosenzweig, M. Parry, Potential impact of climate-change on world food supply, Nature 367 (1994) 133–138.
[4] D. Marks, J. Kimball, D. Tingey, T. Link, The sensitivity of snowmelt processes to climate conditions and forest cover during rain-on-snow: a case study of the 1996 Pacific Northwest flood, Hydrol. Process. 12 (1998) 1569–1587.
[5] A. Hamlet, D. Lettenmaier, Effects of climate change on hydrology and water resources in the Columbia river basin, J. Am. Water Resour. Assoc. 35 (1999) 1597–1623.
[6] C. Barranguet, J. Kromkamp, J. Peene, Factors controlling primary production and photosynthetic characteristics of intertidal microphytobenthos, Mar. Ecol. Prog. Ser. 173 (1998) 117–126.
[7] M. Bertness, G. Leonard, The role of positive interactions in communities: lessons from intertidal habitats, Ecology 78 (1997) 1976–1989.
[8] H. Charles, J.S. Dukes, Effects of warming and altered precipitation on plant and nutrient dynamics of a new england salt marsh, Ecol. Appl. 19 (2009) 1758–1773.
[9] M. Pascual, M. Bouma, A. Dobson, Cholera and climate: revisiting the quantitative evidence, Microbes Infect. 4 (2002) 237–245.
[10] J. Patz, D. Campbell-Lendrum, T. Holloway, J. Foley, Impact of regional climate change on human health, Nature 438 (2005) 310–317.
[11] C. Adami, Self-organized criticality in living systems, Phys. Lett. A 203 (1995) 29–32.
[12] P. Bak, M. Paczuski, Complexity, contingency, and criticality, Proc. Natl. Acad. Sci. USA 92 (1995) 6689–6696.
[13] H.J. Jensen, Self-Organized Criticality: Emergent Complex Behavior in Physical and Biological Systems, in: Cambridge Lecture Notes in Physics, Cambridge University Press, Cambridge, UK, New York, NY, USA, 1998.
[14] S. Redner, A Guide to First Passage Processes, Cambridge University Press, Cambridge, UK, 2001.
[15] A.R. Bulsara, S.B. Lowen, C.D. Rees, Cooperative behavior in the periodically modulated Wiener process: noise-induced complexity in a model neuron, Phys. Rev. E 49 (1994) 4989–5000.
[16] A.R. Bulsara, S.B. Lowen, C.D. Rees, Reply to coherent stochastic resonance in the presence of a field, Phys. Rev. E 52 (1995) 5712–5713.
[17] L. Gammaitoni, P. Hanggi, P. Jung, F. Marchesoni, Stochastic resonance, Rev. Modern Phys. 70 (1998) 223–287.
[18] M. McDonnell, N. Stocks, C. Pearce, D. Abbott, Stochastic Resonance: From Suprathreshold Stochastic Resonance to Stochastic Signal Quantization, Cambridge University Press, Cambridge, UK, 2008.
[19] W. Feller, An Introduction to Probability Theory and its Applications, 3rd ed., vol. 2, Wiley, 1971.
[20] C. Kim, P. Talkner, E.K. Lee, P. Haenggi, Rate description of Fokker–Planck processes with time-periodic parameters, Chem. Phys. 370 (2010) 277–289.
[21] P. Jung, Periodically driven stochastic-systems, Phys. Rep. 234 (1993) 175–295.
[22] P. Talkner, L. Machura, M. Schindler, P. Hanggi, J. Luczka, Statistics of transition times, phase diffusion and synchronization in periodically driven bistable systems, New J. Phys. (2005) 7.
[23] M. Schindler, P. Talkner, P. Hanggi, Escape rates in periodically driven Markov processes, Physica A 351 (2005) 40–50.
[24] A. Polyanin, Handbook of Linear Partial Differential Equations for Engineers and Scientists, Chapman and Hall/CRC, New York, NY, USA, 2002.
[25] D.R. Cox, H.D. Miller, The Theory of Stochastic Processes, Chapman & Hall, CRC, Boca Raton, Florida, USA, 1965.
[26] H. Daniels, Sequential tests constructed from images, Ann. Statist. 10 (1982) 394–400.
[27] V. Lo, G. Roberts, H. Daniels, Sequential tests constructed from images, Bernoulli 8 (2002) 53–80.
[28] M. Abramowitz, I.A. Stegun, Handbook of Mathematical Functions with Formulas, Graphs, and Mathematical Tables, ninth dover printing, tenth GPO printing ed., Dover, New York, 1964.
[29] N. Johnson, S. Kotz, N. Balakrishnan, Continuous Univariate Distributions, vol. 1, Wiley and Sons, New York, USA, 1994.
[30] P. Gaspard, X. Wang, Sporadicity—between periodic and chaotic dynamical behaviors, Proc. Natl. Acad. Sci. USA 85 (1988) 4591–4595.
[31] A. Molini, G.G. Katul, A. Porporato, Revisiting rainfall clustering and intermittency across different climatic regimes, Water Resour. Res. 45 (2009).
[32] J.R. Rigby, A. Porporato, Precipitation, dynamical intermittency, and sporadic randomness, Adv. Water Resour. 33 (2010) 923–932.

[33] T. Barnett, R. Malone, W. Pennell, D. Stammer, B. Semtner, W. Washington, The effects of climate change on water resources in the west: introduction and overview, Clim. Change 62 (2004) 1–11.
[34] T.P. Barnett, J.C. Adam, D.P. Lettenmaier, Potential impacts of a warming climate on water availability in snow-dominated regions, Nature 438 (2005) 303–309.
[35] T.P. Barnett, D.W. Pierce, Sustainable water deliveries from the Colorado river in a changing climate, Proc. Natl. Acad. Sci. USA 106 (2009) 7334–7338.
[36] P. Perona, P. D'Odorico, A. Porporato, L. Ridolfi, Reconstructing the temporal dynamics of snow cover from observations, Geophys. Res. Lett. 28 (2001) 2975–2978.
[37] N.C. Pepin, J.D. Lundquist, Temperature trends at high elevations: patterns across the globe, Geophys. Res. Lett. 35 (2008).
[38] Q.L. You, S.C. Kang, N. Pepin, W.A. Flugel, Y.P. Yan, H. Behrawan, J. Huang, Relationship between temperature trend magnitude, elevation and mean temperature in the tibetan plateau from homogenized surface stations and reanalysis data, Glob. Planet. Change 71 (2010) 124–133.
[39] D. De Walle, A. Rango, Principles of Snow Hydrology, Cambridge University Press, Cambridge, UK, 2008.
[40] R.L. Bras, Hydrology: An Introduction to Hydrological Science, Addison-Wesley, Reading, MA, 1990.